Electrochimica Acta, 1972, Vol. 17, pp. 901 to 913. Pergamon Press. Printed in Northern Ireland

THE ANODIC BEHAVIOUR OF NICKEL IN MOLTEN SODIUM-NITRATE–POTASSIUM-NITRATE EUTECTIC*

A. J. ARVÍA, R. C. V. PIATTI and J. J. PODESTÁ
Instituto Superior de Investigaciones, División Electroquímica, Facultad de Ciencias Exactas, Universidad Nacional de La Plata, La Plata, Argentina

Abstract—The kinetic behaviour of nickel anodes immersed in molten sodium-nitrate–potassium-nitrate eutectic has been investigated in the temperature range 244–314°C, with steady and non-steady electrochemical methods.

The metal passivates by formation of a NiO layer of an average thickness 11 Å. A characteristic passivation potential is established, probably associated to a mixed potential, the over-all reaction being

$$2(Na, K)NO_3 + Ni = NiO + 2NO_2 + (Na, K)_2O.$$

Beyond the passivity region the dissolution of the passive film occurs, at an anode potential where both NO_3^- and oxide ions are able to discharge. The likely over-all electrochemical processes are envisaged with the aid of potential/pO^{2-} diagrams. The considerably changing electrode roughness make a mechanistic interpretation of the anodic processes very uncertain at present.

Résumé—Etude, dans l'intervalle de températures compris entre 244 et 314°C et au moyen de techniques électrochimiques stationnaires et non stationnaires, du comportement cinétique des anodes de nickel immergées dans l'eutectique fondu nitrate de sodium-nitrate de potassium.

Le métal se passive par formation d'une couche de NiO d'une épaisseur moyenne de 11 Å. Un potentiel caractéristique de la passivation s'établit, probablement associé à un potentiel mixte, la réaction globale étant

$$2(Na, K)NO_3 + Ni = NiO + 2NO_2 + (Na, K)_2O.$$

Au delà de la région de passivité, la dissolution du film passif apparaît, à un potentiel anodique où à la fois NO_3^- et les ions de l'oxyde sont susceptibles de se décharger. Les processus électrochimiques globaux vraisemblables sont envisagés à l'aide des diagrammes potentiel/pO^{2-}. La rugosité de l'électrode variant de façon considérable, rend, pour l'instant, l'interprétation du mécanisme des processus anodiques très incertaine.

Zusammenfassung—Das kinetische Verhalten von Nickelanoden in eutektischen Schmelzen von Natrium- und Kaliumnitrat wurde bei Temperaturen zwischen 244 und 314°C untersucht. Das Metall passiviert durch die Bildung einer Schicht von NiO mit einer mittleren Dicke von 11 Å. Es stellt sich ein charakteristisches Passivierungspotential ein, das wahrscheinlich mit einem Mischpotential verknüpft ist, wobei folgende Globalreaktion abläuft

$$2(Na, K)NO_3 + Ni = NiO + 2NO_2 + (Na, K)_2$$

Ausserhalb des passiven Gebietes löst sich die Schicht auf, und zwar bei einem anodischen Potential, bei welchem NO_3^- wie auch Oxydionen entladen werden können. Die möglichen elektrochemischen Gesamtprozesse werden mit Hilfe von Potential/pO^{2-}-Diagrammen ermittelt. Vorläufig macht die sich beträchtlich ändernde Oberflächenrauhigkeit der Elektrode eine mechanistische Interpretation der anodischen Vorgänge sehr ungewiss.

INTRODUCTION

THE ELECTROCHEMICAL behaviour of nickel anodes in alkali-nitrate melts has been the subject of various publications. Thus, Gurovich[1] obtained corrosion data for nickel and other metals and alloys by studying the weight change after short immersion of the samples in alkali-nitrate melts at 400–500°C. Piontelli *et al*[2] studied the passivation of nickel in the eutectic $NaNO_3$–KNO_3 and determined by X-ray diffractometry the

* Manuscript received 31 March 1971.

formation of NiO. Swofford and Laitinen,[3] from the residual-current/voltage curves for solid nickel microelectrode in the eutectic at 250°C, observed chemical attack and an erratic trace on anodic polarization. Brough and Kerridge[4] studied the reaction of several metals in the same system, reporting reactions to start above 500°C, but the reaction products were not identified. Conte and Casadio studied the electrochemical behaviour of several metals in molten alkali nitrates, trying to correlate the qualitative information with simple potential/pO^{2-} diagrams, and also performing some potentiodynamic experiments to get more information about this system.[5–8]

The present work attempts to contribute to the kinetics of nickel passivation and dissolution of passive nickel electrodes in alkali-nitrate melts, as well as to the knowledge of the cause of passivation of nickel in these melts.

EXPERIMENTAL TECHNIQUE

The experimental set-up, including electrode materials and measuring circuitry, was the same as previously described for the study of the electrochemical behaviour of iron and nickel anodes in molten nitrites.[9–10] In these experiments three different reference electrodes were indiscriminately used, (i) a $Ag/AgNO_3$(m) eutectic, (ii) a nitrate electrode and (iii) a platinum electrode dipped into the alkali-nitrate melt. The latter was, however, preferentially employed, since it gives an arbitrary reference potential which in a simpler manner reproduces equally well that of the nitrate electrode.

The electrolyte was a $NaNO_3$–KNO_3 melt having the eutectic composition (50–54·5-mol respectively), and mp 218–222°C.

Conventional analytical methods were employed for the faradaic yields, and X-ray diffractometry for the determination of the structure of nickel oxide formed during the anodic polarization.

Experiments were run in the temperature range from 244–314°C using both partially dehydrated and vacuum-dehydrated alkali-nitrate melts.

RESULTS

The electrode potential at null current

Once the metal is immersed in the molten salt its potential lies at about —0·3 V with respect to the reference potential and steadily becomes more positive until it finally attains, after 4 h at 270°C, a potential of —0·175 V. If the electrode is now anodically polarized with an overpotential of 0·025 V for a few minutes, and then the current is interrupted, the potential returns to —0·175 V. The situation, however, is completely different after anodic polarization at about 0·5 V above the immersion potential. In this case, after current interruption, the rest potential is significantly more positive, being about 0·15 V. The difference between the first and the second rest potentials, as shown in Table 1, is independent of temperature.

Current/potential curves

(a) *Potentiostatic runs.* Figures 1–3 show typical potentiostatic E/log i curves obtained with the vacuum-dehydrated melt at different temperatures. The runs were initiated by changing the potential of freshly polished nickel electrodes from

TABLE 1. KINETIC PARAMETERS DERIVED FROM POTENTIOSTATIC E/log i PLOTS. DEHYDRATED MELTS

Temp °C	E_p V	E_r V	$(E_p - E_r)$ V	log $(i_p)_M$ i, μA/cm²	log $(i_p)_m$ i, μA/cm²	$(b_T)_a$ V	log $(i_0)_{E_r}$ i, μA/cm²
233	−0·230	0·150	0·380	0·86	−0·10	0·235	2·96
251	−0·210	0·155	0·365	1·46	0·07	0·245	3·14
259	−0·210	0·160	0·370	1·68	0·74	0·215	3·16
274	−0·165	0·210	0·375	1·60	0·16	0·215	3·36
305	—	0·250	—	—	—	0·225	3·72

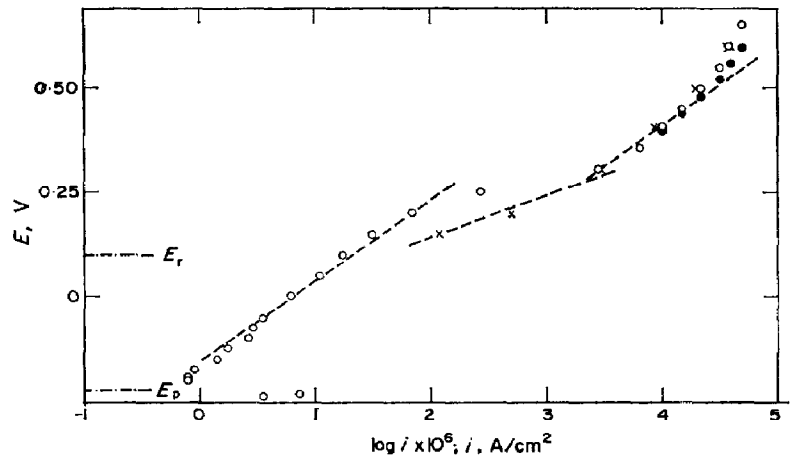

FIG. 1. Semilogarithmic plot of a potentiostatic E/i curve. Dehydrated melt. 233°C. ○, anodic potential increase; ×, anodic potential decrease; ●, data corrected for pseudo-ohmic polarization.

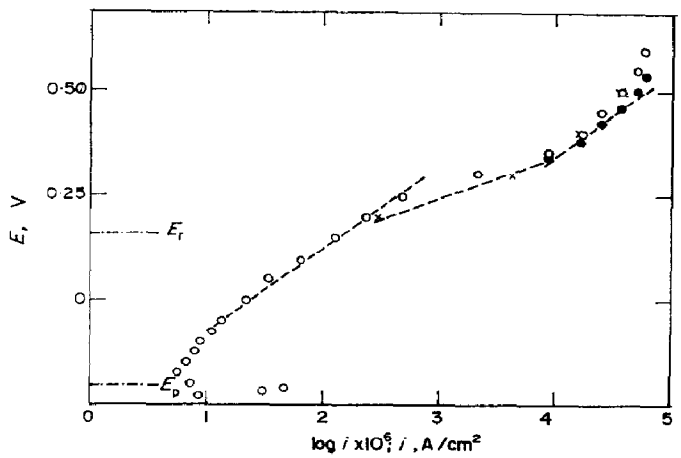

FIG. 2. Semilogarithmic plot of a potentiostatic E/i curve. Dehydrated melt. 259°C. ○, anodic potential increase; ×, anodic potential decrease; ● data corrected for pseudo-ohmic polarization.

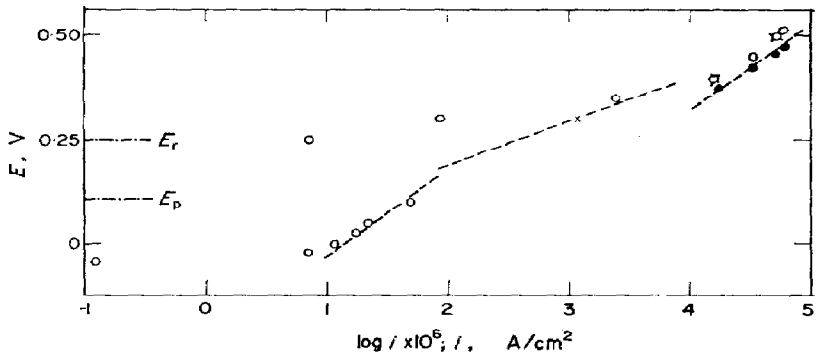

FIG. 3. Semilogarithmic plot of a potentiostatic E/i curve. Dehydrated melt, 305°C. ○, anodic potential increase; ×, anodic potential decrease; ●, data corrected for pseudo-ohmic polarization.

their immersion value upward, and then recording E/I data by changing the potential in the reverse direction. The $E/\log i$ characteristic exhibits the same particular features over the whole range of temperature investigated. Thus, a small increase of the electrode potential from its value at immersion causes the cd to increase rapidly up to a maximum value, $(i_p)_M$, where a definite passive state of the nickel electrode is achieved. Then, at the passivation potential, E_p, the cd decreases to a minimum value, $(i_p)_m$, which is about ten times lower than the maximum. A further potential increase causes a cd increase and the relationship between E and $\log i$ in this region apparently approaches a Tafel line with a slope, $(b_T)_1$, $2{\cdot}3(2RT/F)$, over nearly two decades of cd. When the potential reaches about 0·4 V above the passivation potential, depolarization of the electrode occurs. This is clearly shown, for instance at 233°C, where a potential change of 0·1 V increases the current about ten times. The Tafel line in this region has a slope, $(b_T)_2$, close to $2{\cdot}3(RT/F)$. By increasing the potential still further, another Tafel line portion occurs, with a slope, $(b_T)_3$, again close to $2{\cdot}3(2RT/F)$.

By running the potentiostatic curve in reverse the portions which clearly reproduce those of the curve described above are the Tafel regions observed at high anode potentials and the depolarization region. The rest potential, E_r, then attained is located about 0·35 V more positive than the passivation potential. If the experiment is continued by running a second E/I curve with the same electrode starting from the rest potential, the curve is reproduced according to the description already given for the returning curve.

Parameters derived from $E/\log i$ plots are assembled in Table 1. $(i_0)_{E_r}$ is an apparent cd extrapolated to E_r, according to the Tafel line of slope $(b_T)_3$.

Potentiostatic E/I curves were also recorded by using a melt which was not vacuum-dehydrated. The $E/\log i$ curves are closely coincident with those already reported for the vacuum dehydrated melt, Table 2. Potentiostatic runs made with electrodes previously dipped in the melt for a long period (16 h) yield the upper part of the E/I curve, starting from the rest potential. The returning curve also exhibits a marked hysteresis which is probably related to the change of electrode area due to corrosion of the sample. As before, the passivation effect is greatly enhanced at temperatures above 300°C. The effect of water is, in principle, similar to that observed for the nickel anodes in nitrite melts.[9]

TABLE 2. KINETIC PARAMETERS DERIVED FROM POTENTIOSTATIC E/log i PLOTS. UNDEHYDRATED MELT

Temp °C	E_p V	E_r V	$(E_p - E_r)$ V	log $(i_p)_M$ i, μA/cm²	log $(i_p)_m$ i, μA/cm²	$(b_T)_a$ V	log $(i_0)_{E_r}$ i, μA/cm²
244	−0·150	0·200	0·350	1·94	0·86	0·225	3·20
244	−0·150	0·210	0·360	1·33	1·20	0·230	3·14
251	−0·110	0·240	0·350	1·58	1·20	0·265	3·16
268	−0·150	0·210	0·360	1·73	1·35	0·180	3·10
275	−0·090	0·270	0·360	1·80	0·07	0·180	3·32
314	−0·135	0·300	0·435	—	—	0·200	3·70

Galvanostatic E/I *curves*

A typical galvanostatic E/log i curve is shown in Fig. 4. The initial portion of the plot is characterized by potential instability and no reliable steady data can be obtained, except beyond the rest potential value.

At a constant cd, the potential reaches the value of the passivation potential and remains there for a certain time depending on the value of i. Then a jump of potential occurs, to attain a value of 0·35 V or more above the passivation potential. The portion of the curve extending beyond that value coincides reasonably well with

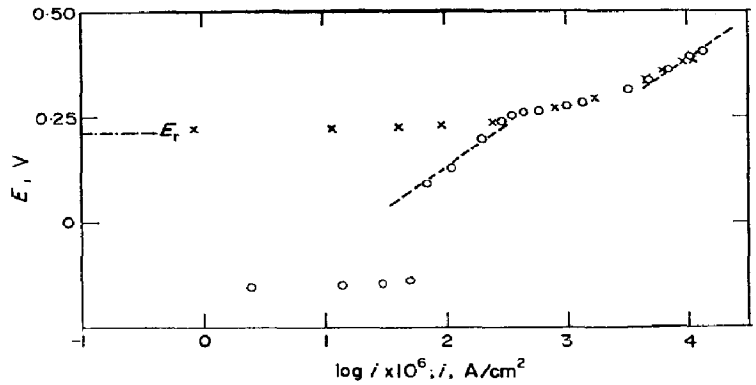

FIG. 4. Semilogarithmic plot of a galvanostatic E/i curve. Dehydrated melt. 263°C.
○, anodic potential increase; ×, anodic potential decrease.

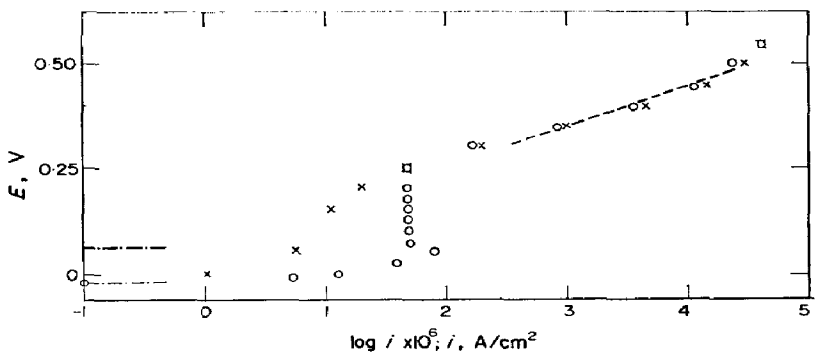

FIG. 5. Semilogarithmic plot of a potentiostatic E/i curve in the presence of 0·2 m $NaNO_3$. 260°C.
○, anodic potential increase; ×, anodic potential decrease.

potentiostatic data. Results derived from the galvanostatic curves are assembled in Table 3.

TABLE 3. DATA DERIVED FROM GALVANOSTATIC E/log i CURVES

Temp °C	E_p V	E_r V	$(E_p - E_r)$ V	$(b_T)_3$ V	log $(i_0)_{E_r}$ i_0, μA/cm^2
247	−0·150	0·210	0·360	0·190	2·86
268	−0·155	0·210	0·365	0·210	3·14
290	−0·140	0·240	0·380	—	—

E/I *curves with addition of* $NaNO_2$

Potentiostatic E/I curves were also obtained after addition of $NaNO_2$ to the original eutectic. Figures 5 and 6 show semilogarithmic plots of polarization curves

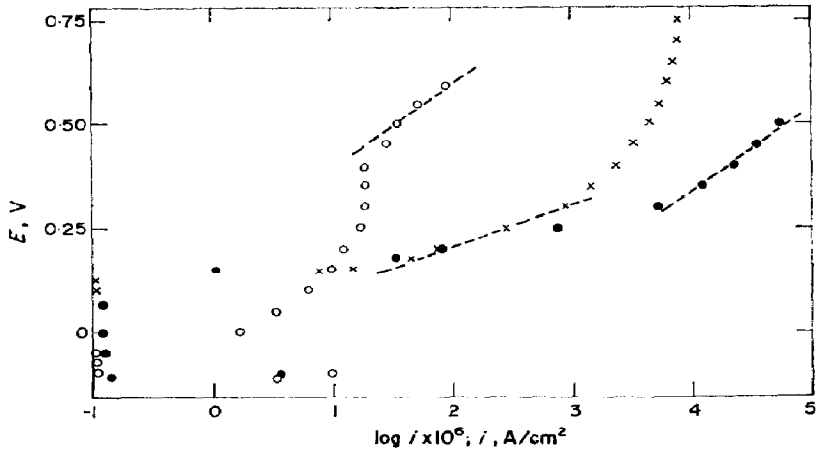

FIG. 6. Semilogarithmic plots of potentiostatic E/i curves in the presence of $NaNO_2$. 275°C
○, iron anode in the original melt, containing $NaNO_2$ as initial impurity; ×, iron anode in the original melt with addition of 0·12 m $NaNO_2$; ●, nickel anode in the same melt.

obtained in the presence of $NaNO_2$, potentiostatically determined by changing the potential first upward and then downward. As is known, the thermal decomposition of the melt yields nitrite, and its presence is evidenced by the usual appearance of a current plateau in the E/I curves at potential lower than those where the nitrate melt undergoes electrochemical decomposition. This limiting cd was clearly established[10] for the case of iron anodes, but not for nickel. To confirm the absence of the nitrite oxidation limiting current, experiments with addition of nitrite to the melt were performed, and furthermore, to assess the existence of the limiting current, the same melt was electrolysed by repeating the experiments with iron anodes. These experiments clearly confirmed the potential region where the nitrite-ion discharge takes place and the different behaviour of nickel and iron electrodes in these melts.

Macroscopic observations

The macroscopic aspect of the metal depends on the electrolysis conditions. A bright clean surface electrode at 270°C, under a cd of 1 $\mu A/cm^2$ for 15 min, exhibits a straw-coloured surface. The same experiment performed potentiostatically, at 150 $\mu A/cm^2$, in the region where the first Tafel slope appears, yields an apparently clean electrode surface. If the nickel anode is polarized in the depassivation region at 2·5 mA/cm^2, it turns bright again as if the electrode has been electropolished. Finally, electrolysis at higher anode potentials, with apparent cds of the order of 25 mA/cm^2, gives evolution of gases and the formation of a rather thick poorly adherent black NiO film.

Faradaic yields

The reaction products involve the formation of nitrogen oxides, principally nitrogen dioxide, nickelous ions in the melt, and the precipitation of NiO. The total amount of corroded nickel, either as NiO or as soluble nickel in the melt, was determined, at 275°C and 100 $\mu A/cm^2$, after a 5-day electrolysis. The faradaic yield, assuming $2F$ per mole of nickel, was practically 100 per cent. At 20 mA/cm^2, the experiment yields a similar result, but soluble nickel ion clearly predominates, since the Ni^{2+}/NiO ratio is 6:1.

Some additional experiments to determine any spontaneous dissolution or chemical reaction of black NiO in the melt were made. One per cent NiO was added to the eutectic melt, at 250°C. Colorimetric analysis for nickel ion in the melt, after separation of NiO and dissolution in water, gave a negative result. The same result was also obtained in the presence of NO_2.

X-ray diffractograms

X-ray diffractograms were obtained for plane plate nickel samples electrolysed at different cds corresponding to the passivity and passive-nickel-dissolution regions. The diffractograms, apart from the characteristic peaks corresponding to $NaNO_3$ and KNO_3, showed the peaks of NiO lattice structure. The diffractograms obtained at low cd exhibited more intense NiO peaks than those run with the nickel samples electrolysed at high cds.

A Debye–Scherer diffractogram made with the black powder separated from the melt after electrolysis at high cd, also gave the NiO lattice structure.

Decay of anode potential at current interruption

The anode potential decay, as shown in semilogarithmic plots in Fig. 7, depends on the potential where the current was switched off, on the temperature and on the presence of nitrite ion in the melt. In the figures the overpotential, η, is defined as $E - E_p$.

At low temperature, with melts without addition of nitrite to the amount it contains due to the thermal decomposition, the $E/\log t$ plot exhibits the usual shape; that is, at $t \to 0$, it approaches asymptotically the initial electrode potential after correction for the pseudo-ohmic drop. Similarly as $t \to \infty$, the electrode potential attains a constant value. The latter, however, depends on the region of the steady E/I curve corresponding to electrolysis interruption. Thus, if the current is switched off in the region of the E/I curve preceding the depassivation region, the potential

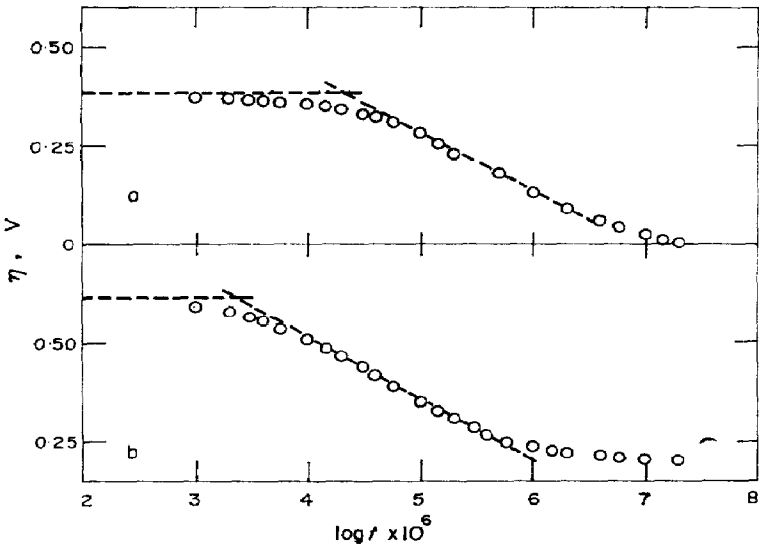

FIG. 7. Semilogarithmic plots of the anode potential decay. 250°C. a, 13·5 μA/cm²; b, 99 μA/cm². t in s.

approached at $t \rightarrow \infty$ is the passivation potential, but if the interruption occurs beyond the depassivation region, then the attained potential is close to the rest potential of the nickel anode. Furthermore, this is always the rest potential obtained for decay experiments at temperatures above 290°C.

The middle portion of the E/log t plot fits a straight line over two log (time) decades or thereabouts. The decay slope, b_d, diminishes as temperature increases. These slopes, however, have to be considered differently according to the final potential attained by the electrode at current interruption. Kinetic data derived from the decay curves of anodic potential are assembled in Table 4. η_i is the overpotential at current interruption; log t' is obtained by extrapolating the straight line at η_i; C is the apparent electrode differential capacitance and η_t is the overpotential at $t \rightarrow \infty$.

Galvanostatic build-up of anode potential

When a freshly polished nickel electrode is used, the galvanostatic build-up of anode potential exhibits an E/t pattern involving a net transition time. The electrode response in this case is very similar to that already analysed for that electrode in alkali-nitrite melts.[9] The potential at $\tau_{1/4}$ is close to the passivation potential, but its determination is less accurate than in the case of the alkali-nitrite melts, through the uncertainty of the initial potential for rapid spontaneous passivation that nickel undergoes in molten nitrates. The transition time is no longer observed when passivated electrodes are employed.

The product $i\tau$, where τ is the galvanostatic build-up transition time, is constant in the current range investigated. The average maximum quantity of electricity obtained on freshly polished samples is 2·0 mC/cm². This corresponds to an average passive film thickness at the passivation potential of 11 Å, assuming that its composition is NiO, as earlier reported.[2]

TABLE 4. KINETIC DATA DERIVED FROM ANODIC POTENTIAL DECAY

η_i V	i $\mu A/cm^2$	log (t') t, μs	b_a V	C $\mu F/cm^2$	η_t V
		240°C			
0·335	92	4·90	0·165	102·0	0
0·412	460	4·37	0·170	146·0	0
0·440	1326	4·00	0·150	204·0	0
0·450	1840	4·05	0·135	355·0	0
0·500	5100	3·90	0·145	643·0	—
0·680	12420	4·11	0·180	2050·0	0·320
		250°C			
0·383	99	4·32	0·150	32·2	0
0·400	385	3·87	0·115	57·0	0
0·460	1430	3·67	0·135	114·0	0
0·610	13500	3·36	0·155	460·0	0·200
		260°C			
0·330*	13800	3·40	0·085	940·0	0
0·400	115	4·10	0·155	21·5	0
0·445	1035	3·58	0·125	79·5	0
0·535	9200	3·20	0·145	232·0	0·200
0·585	14000	3·78	0·165	1180·0	0·275
		271°C			
0·305	99	4·50	0·160	45·1	0
0·340	220	4·38	0·140	87·0	0
0·405	495	4·25	0·135	150·0	0·100
0·430	1430	3·76	0·115	165·0	0·250
0·525	13400	3·63	0·110	1197·0	0·330
		309°C			
0·460	92	4·40	0·073	73·0	0·325
0·470	356	3·84	0·085	67·0	0·300
0·480	12380	3·35	0·085	750·0	0·305

* Experiment with the addition of nitrite ion.

DISCUSSION

Nickel anodes in the alkali-nitrate eutectic melts exhibit, under steady potentiostatic polarization, an E/I characteristic showing, when the electrode is used for the first time, a typical current peak corresponding to the onset of passivity. This region disappears when a galvanostatic run is made. At high anode potentials other processes take place provoking corrosion of the metal either to NiO or Ni^{2+} ion.

The characteristic potential arrests observed for the nickel anodes in this melt resembles, at least in part, the previous description of the electrochemical processes occurring with iron anodes in the same eutectic.[11] Consequently, it seems reasonable, in order to identify the over-all reactions which prevail in the system from the thermodynamic viewpoint, to compare the potential arrests already described, with the potential/pO^{2-} diagram for nickel in sodium nitrate. This diagram has been calculated some time ago[5] and a more recent version of it is available containing more information over a larger temperature range.[12] It has been built on the basis that NiO is the only stable nickel oxide at the temperature of the molten alkali nitrates.

The present work confirms that the film that characterizes the passive region has the NiO lattice structure, although the possibility exists of having non-stoichiometric nickel oxides, with a higher oxygen content at higher potentials. Nickel undergoes spontaneous passivation in the nitrate melt, as is revealed by the continuous shift of the electrode potential from the value acquired on immersion towards a

more positive value closer to the passivity potential, with the simultaneous formation of a nickel-oxide film, which at this stage has a straw colour. As recently reported, the idea of a monolayer of oxide would in this case be related to the beginning of passivation.[14]

The average thickness of nickel oxide involved at the onset of passivity, according to galvanostatic transients, is of the order of 11 Å, a figure very close to that already mentioned for nickel anodes in alkali-nitrite melts. The passivation process takes place much faster than in the case of nitrite melts, probably due to the higher oxidizing power exhibited by molten nitrates.

The spontaneous passivation, as deduced from the potential/pO^{2-} diagram,[12] can be considered as the sum of the following two reactions, one due to solvent reduction and the other due to metal oxidation,

$$NO_3^- + e = NO_2 + O^{2-} \quad (1)$$

and

$$Ni + O^{2-} = NiO + 2\,e. \quad (2)$$

The over-all reaction occurring at a mixed potential, E_m, is

$$2(Na, K)NO_3 + Ni = NiO + 2NO_2 + (Na, K)_2O. \quad (3)$$

The mixed potential is probably located very close to the passivation potential, and it can be calculated as follows with respect to the reversible nitrate electrode. Let us take the activities of NO_3^-, NO_2, Ni and NiO equal to unity, and for this eutectic, assume that the molar oxide-ion concentration[13] is $8{\cdot}2 \times 10^{-12}$. As the standard potential of these reactions are known ($E_1 = -0{\cdot}876$ V and $E_2 = 1{\cdot}42$ V),[12] the mixed potential, with respect to nitrate electrode, is $E_m = -1{\cdot}96$ V and $pO^{2-} = 13{\cdot}1$ at the electrode interface.

The passivity region extends over a potential range of about 0·35 V. The potentiostatic E/I curve exhibits there an apparent Tafel relationship the meaning of which is quite uncertain, as in the case of nickel anodes in molten alkali nitrites.[9] This region, where, as reported, the curves were erratic,[3] can be explained in terms of non-steady results, particularly those obtained from the decay of anode overpotential. The $E/\log t$ patterns were always obtained after a steady current had been attained at the electrode at a constant potential and, as shown in Table 4, the apparent electrode differential capacitance depends either on the initial electrolysis current or on the electrode potential at which decay initiates. If the lowest capacitance is arbitrarily assumed to correspond to an even, smooth surface and its increase either with current or potential is attributed to an increase of electrode roughness, their ratio will supply an idea about the electrode surface change in the passivation region. The result of this correction, for instance at 240°C (Fig. 8), shows that the cd in the passivation region is practically potential-independent as has already been observed for passivation phenomena in aqueous solutions. A current due to dissolution of the passive film exists which would be, as in the case of alkali nitrite melts,[9] independent of potential within the passivity region, having a probable value given by the smallest apparent current density obtained just when the passivation potential has been reached. This current density should correspond to a chemical reaction which can probably be explained in the same way as in the case of nickel anodes in molten alkali nitrites.[9]

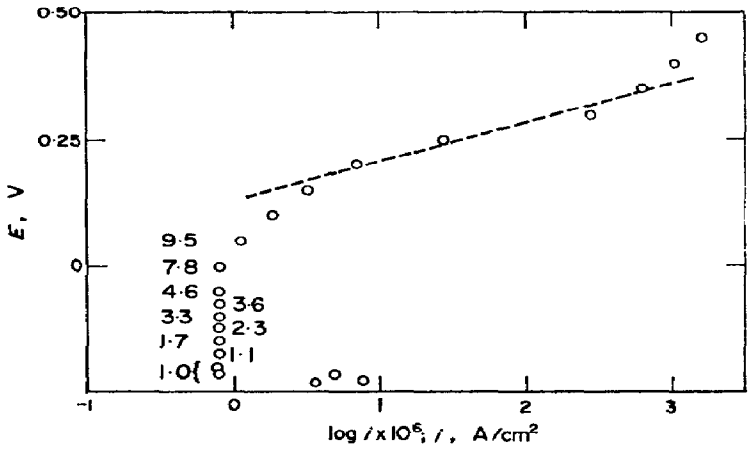

FIG. 8. Semilogarithmic plot of a potentiostatic E/i curve after correction for roughness factors estimated from the apparent electrode differential capacitances. These factors are given in the figure. Dehydrated melt. 233°C

When the potential is about 1 V more positive than the passivity potential, a relatively rapid rate of current increase with potential occurs, indicating that a new electrode process takes place at the electrochemical double layer. When no particular amounts of nitrite ions are added to the melt, the region where the passive metal is dissolved covers no more than one logarithmic decade of cd, and no clearcut E/I relationship can be established. However, when sodium nitrite is added to the melt, this region extends appreciably, covering, for the data illustrated in Figs. 6 and 7, nearly two decades. There a Tafel line having a slope equal to RT/F can be drawn as was the case for experiments run with the alkali nitrite melt.[9]

It is predictable from the E/pO^{2-} diagram, that after approximate corrections for the activities of substances participating in the reactions, at about 1 V above the passivation potential the nitrite-ion discharge proceeds. Consequently, the same reaction pathway already discussed recently for passive nickel dissolution in molten alkali nitrites[9] should apply also in this potential region for the passive nickel dissolution in molten alkali nitrates. Another interesting fact, however, is that no limiting current is observed when nickel electrodes are used, so that it appears as if no convective-diffusion control exists in this case, a fact which is rather peculiar and whose explanation can be attempted. The simplest interpretation of this effect is that it may be related to a relatively large actual area increase of the nickel electrode. This explanation is sustained by the increase of the apparent differential electrode capacitance by a factor of nearly 10 with respect to the apparent electrode capacitance obtained in the cd region where the limiting current exists for the case of iron anode.[9] Another perhaps more realistic possibility involves the occurrence of a different process at a potential close to that corresponding to the nitrite electrode in the melt.[12] This reaction might, for instance, be the discharge of oxide ions according to

$$O^{2-} = \tfrac{1}{2}O_2 + 2\,e. \qquad (5)$$

The occurrence of this reaction served to explain the abrupt depassivation observed for the case of the iron electrodes in the alkali-nitrate melts.[11] Its occurrence in this potential region will be favoured by the increase of oxide-ion concentration due to

reaction between NO_2 and NO_2^- ion according to

$$NO_2^- + NO_2 = NO_3^- + NO. \quad (6)$$

Therefore, the equilibrium (1) shifts toward O^{2-} formation at the electrochemical double layer. Reaction (6) also explains the formation of NO as one of the reaction products.

Reaction (5) probably plays an important role at high current densities, further contributing to passive nickel dissolution as NiO. This region approaches a slope $2RT/F$ in the $E/\log i$ plot, but this slope is not observed when sodium nitrite is added to the melt. It is therefore plausible that the above mentioned Tafel line has no kinetic significance for some particular process. If this is the case, some additional kinetic parameters are required for an unambiguous interpretation.

The results indicate that larger amounts of soluble nickel are yielded at the highest anode potentials reached in the present work. In this region the occurrence of Ni^{2+} species at high anode potentials is thermodynamically favoured.[12] Its formation can be accomplished after assuming, as in the case of nickel/molten-nitrite,[9] that the passive nickel surface is covered by adsorbed (NO_2). Then the following electrode reaction may occur,

$$NiO(NO_2) = Ni^{2+} + NO_3^- + e. \quad (7)$$

From the kinetic standpoint reaction (7) may predominate at high anode potentials on the passive nickel surface completely covered by (NO_2). Under these circumstances, if step (7) is rate-controlling, it justifies the Tafel slope equal to $2RT/F$ obtained in this potential region.

Finally, when the E/I curve is traced by changing the potential downward, the rest potential of the system lies at 0·350 V above the passivity potential. If the same interpretation advanced on the basis of nickel oxides of different stoichiometry,[15,16] for the nickel rest potential in the nitrite melt is extended to this system, it is concluded that the nickel oxide related to the rest potential has on the average the composition $NiO_{1.36}$. As is known, when Ni and NiO are in contact with oxygen they can first chemisorb and later incorporate relatively large amounts of oxygen. For NiO a phase change occurs and the colour of the oxide changes to black.[17,18] With increasing oxygen content the conductivity of the non-conducting NiO increases, but the lines of NiO can only be detected with X-rays. The material becomes more nearly amorphous with increasing oxygen content.[19]

Acknowledgement—The authors are indebted to the Consejo Nacional de Investigaciones Científicas y Técnicas for partial financial support of the present work. J. J. P. acted as a part-time member of the Departamento de Ingeniería Química de la Universidad Nacional de La Plata.

REFERENCES

1. E. I. GUROVICH, *Zh. prikl. Khim.* **29**, 1358 (1956).
2. R. PIONTELLI, U. BERTOCCI and G. STERNHEIM, *Z. Elektrochem.* **62**, 772 (1958).
3. H. S. SWOFFORD and H. A. LAITINEN, *J. electrochem. Soc.* **110**, 814 (1963).
4. B. J. BROUGH and D. H. KERRIDGE, *Inorg. Chem.* **4**, 1353 (1965).
5. A. CONTE and S. CASADIO, *Ric. Sci.* **36**, 488 (1966).
6. A. CONTE and S. CASADIO, *Ric. Sci.* **36**, 433 (1966).
7. A. CONTE, *Electrochim. Acta* **11**, 1579 (1966).
8. A. CONTE and S. CASADIO, *Elettroliti e processi electtrochimici*, Chap. 3. Consiglio Nazionale delle Ricerche, Roma (1968).

9. A. J. Arvía, J. J. Podestá and R. C. V. Piatti, *Electrochim. Acta* **16**, 1797 (1971).
10. A. J. Arvía, J. J. Podestá and R. C. V. Piatti, *Electrochim. Acta* **17**, 33 (1972).
11. A. J. Arvía, R. C. V. Piatti and J. J. Podestá, *Electrochim. Acta* **17**, 889 (1972).
12. S. L. Marchiano and A. J. Arvía, *Electrochim. Acta* **17**, 861 (1972).
13. R. N. Kunst and F. R. Duke, *J. Am. chem. Soc.* **85**, 3338 (1963).
14. G. Trusov, E. P. Gochalieva and U. M. Novakovskii, *Elektrokhimiya* **4**, 366 (1968).
15. B. E. Conway and M. A. Sattar, *J. electroanal. Chem.* **19**, 351 (1968).
16. D. Mehandjiev, *C.r. Acad. Bulg. Sci.* **22**, 1253 (1969).
17. M. W. Roberts and B. R. Wells, *Trans. Faraday Soc.* **62**, 1608 (1966).
18. J. Labat, *J. Chim. phys.* **60**, 1251 (1963).
19. J. J. Lander, *Acta Cryst.* **4**, 148 (1951).